Strain Free Ge/GeSiSn Quantum Cascade Laser Based on L-valley Intersubband Transitions

Greg Sun, Jose Menéndez, Jacob B. Khurgin, and Richard A. Soref

***Abstract*— we design a Ge/$Ge_{0.76}Si_{0.19}Sn_{0.05}$ quantum cascade laser that operates at L-valleys of the conduction band with a lasing wavelength of 49 µm. This particular alloy composition gives a "clean" conduction band offset of 150meV at L-valleys with all other energy valleys sitting higher in energy. All QCL layers are lattice matched to a $Ge_{0.76}Si_{0.19}Sn_{0.05}$ buffer layer and therefore strain free. Lifetimes determined from the deformation potential scattering of nonpolar optical and acoustic phonons are at least an order of magnitude longer than those in polar III-V QCLs, reducing threshold current density.**

I. INTRODUCTION

ELECTRICALLY pumped Si-based lasers have long been sought after because they serve as light sources for monolithic integration of Si electronics with photonic components on the same Si wafer. Unfortunately, Si has not been a material of choice for photonic applications owing to its indirect bandgap. It has been proposed that lasers based on intersubband transitions (IST) in SiGe quantum wells (QWs) could circumvent the issue of bandgap indirectness [1]. In addition, SiGe QWs being nonpolar material is expected to have longer intersubband lifetimes reducing threshold current and to be free of reststrahlen band in comparison with III-V quantum cascade lasers (QCLs). Several groups have obtained electro-luminescence from SiGe QWs [2-4], but lasing has eluded researchers up to now. These efforts all have one scheme in common, i.e., holes instead of electrons are used for IST because SiGe QWs have most of its band offset in valence band rather than in conduction band. There are a number of difficulties associated with valence band SiGe QCLs. First, the strong mixing of heavy-hole, light-hole, and split-off bands makes the QCL design exceedingly cumbersome with a great degree of uncertainty. Second, the large effective mass of heavy holes hinders carrier injection efficiency and leads to small ISB oscillator strength between laser states. Third, for any significant band offset necessary for implementing QCLs, lattice-mismatch induced strain in SiGe QWs is likely to generate structural defects. Recently, a new approach was proposed to construct a conduction band SiGe QCL using strained Ge QWs and SiGe alloy barriers [5]. Such a structure effectively avoids the complexity of valence band, but the two Δ_2-valleys along the (001) growth direction are still entangled with the L-valleys in conduction band, potentially creating additional nonradiative decay channels for the upper laser state.

We propose to employ Ge/$Ge_{1-x-y}Si_xSn_y$ heterostructures to develop L-valley QCLs. $Ge_{1-x-y}Si_xSn_y$ alloys have been studied for the possibility of forming direct bandgap semiconductors [6-9]. Since the first successful growth of this alloy [10], relaxed epilayers with a wide range of alloy contents in device quality have been achieved. Incorporation of Sn provides the opportunity to separately engineer strain and band structure since we can vary Si (x) and Sn (y) compositions independently to yield desired lattice constant and band structure. With a proper alloy composition, this material system offers the possibility of a "cleaner" conduction band lineup with L-valleys in both well and barrier sitting below all other valleys (Γ, Δ_2, Δ_4), a light effective electron mass along the (001) growth direction in comparison with that of heavy holes, and a lattice-matched structure that is entirely strain free. In addition, the strain-free QCL can be grown on (001) Si substrate via lattice matched $Ge_{1-x-y}Si_xSn_y$ /Sn_zGe_{1-z} buffer layer [10].

II. LASER STRUCTURE DESIGN

Based on the method previously developed in [9], we have calculated the band lineup in Ge/$Ge_{1-x-y}Si_xSn_y$ heterostructures under the condition that the lattice constant of $Ge_{1-x-y}Si_xSn_y$ alloy matches that of Ge. Our result indicates that a conduction-band offset of 150meV at L-valleys can be obtained between lattice-matched $Ge_{0.76}Si_{0.19}Sn_{0.05}$ alloy and Ge while other conduction-band valleys (Γ, Δ_2, Δ_4) are all above the L-valley band edge of both $Ge_{0.76}Si_{0.19}Sn_{0.05}$ and Ge. This band alignment presents a desirable alloy composition from which a QCL operating at L-valleys can be designed using Ge as QWs and $Ge_{0.76}Si_{0.19}Sn_{0.05}$ as barriers without the complexity arisen from other energy valleys.

Fig.1 shows the QCL structure based on Ge/ $Ge_{0.76}Si_{0.19}Sn_{0.05}$ QWs. Only L-valley conduction-band lineup is shown in the potential diagram under an applied electric field of 10kV/cm. In order to solve the Schrödinger equation to yield subbands and their associated envelope functions, it is necessary to determine the effective mass m_z along the (001) growth direction within the constant-energy ellipsoids at the

G. Sun is with Department of Physics, University of Massachusetts Boston, Boston, MA 02125 USA (phone: 617-287-6432; fax: 617-287-6053; e-mail: greg.sun@ umb.edu).

J. Menéndez is with Department of Physics and Astronomy, Arizona State University, Tempe, Arizona 85287, USA (e-mail: jose.menendez@asu.edu).

J. B. Khurgin is with Department of Electrical and Computer Engineering, The Johns Hopkins University, Baltimore, Maryland 21218, USA (jakek@jhu.edu).

R. A. Soref is with Sensors Directorate, Air Force Research Laboratory, Hanscom AFB, MA 01731 USA (e-mail: Richard.soref@hanscom.af.mil).

L-valleys along (111) direction which is tilted with respect to (001). Using the L-valley principle transverse effective mass $m_t = 0.08 m_o$, and longitudinal effective mass $m_l = 1.60 m_o$ for Ge, we obtain $m_z = (2/3m_t + 1/3m_l)^{-1} = 0.12 m_o$ where m_o is the free electron mass. Magnitude squared of all envelope functions are plotted at relative energy positions of their associated subbands. As shown in Fig.1, each period of the QCL has an active region for lasing emission and an injector region for carrier transport. The active region is constructed with 3 coupled Ge QWs that give rise to three subbands marked 1, 2, and 3 in Fig. 1. Lasing transition at 49 µm is between the upper laser state 3 and lower laser state 2. The depopulation of lower state 2 is through scattering to state 1 and the miniband downstream formed in the injector region which consists of 4 QWs of decreasing well widths all separated by 20Å $Ge_{0.76}Si_{0.19}Sn_{0.05}$ barriers. Another miniband formed of quasi-bound states in the injector region sitting 45 meV above the upper laser state 3 effectively prevents escape of electrons from upper laser state 3 into the injector region. The strong overlap between state 2 and state 1 as well as between state 2 and downstream miniband ensures a fast depopulation of lower laser state.

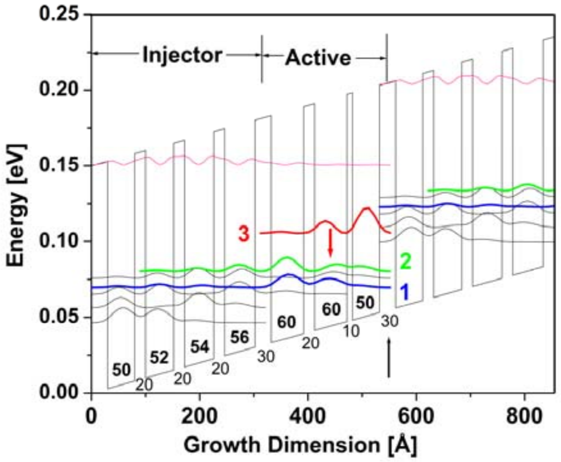

Fig. 1. L-valley conduction band profile and magnitude squared envelope functions plotted at their subband energy positions. Layer thicknesses for one period of the QCL are marked in Å with the injection barrier marked by the arrow.

III. LIFETIMES AND THRESHOLDS

The nonradiative transition rates between different subbands in such a nonpolar material system with a fairly low doping and injection current should be dominated by deformation-potential scattering of nonpolar optical and acoustic phonons. For this Ge-rich structure, we have used bulk-Ge phonons for the calculation of scattering rate to yield lifetimes for upper laser state τ_3 and lower laser state τ_2, as well as 3→2 scattering time τ_{32}. They are shown in Fig. 2 as a function of operating temperature. These lifetimes are at least an order of magnitude longer than those of III-V QCLs owing to the nonpolar nature of GeSiSn alloys. The necessary condition for population inversion $\tau_{32} > \tau_2$ is satisfied throughout the temperature range. Using these lifetimes in population rate equations, we obtain the optical gain of the QCL under injected current density J with injection efficiency η

$$g = \frac{2e^2(\hbar\omega_L)|<3|z|2>|^2}{\varepsilon_o c\hbar n\gamma L_p}[\tau_3(1-\frac{\tau_2}{\tau_{32}})\frac{\eta J}{e} - (\bar{N}_2 - \bar{N}_3)] \quad (1)$$

where $\bar{N}_i$ is the thermal excitation of doping carrier density in subband *i*. We have taken the following values in evaluating the optical gain: the index of refraction n=3.97, lasing transition energy $\hbar\omega_L = 25$ meV, the full width at half maximum $\gamma = 10$ meV, the length of one period of the QCL $L_p = 532$Å, area doping density per period of 10^{10} / cm^2, and injection efficiency $\eta = 1$.

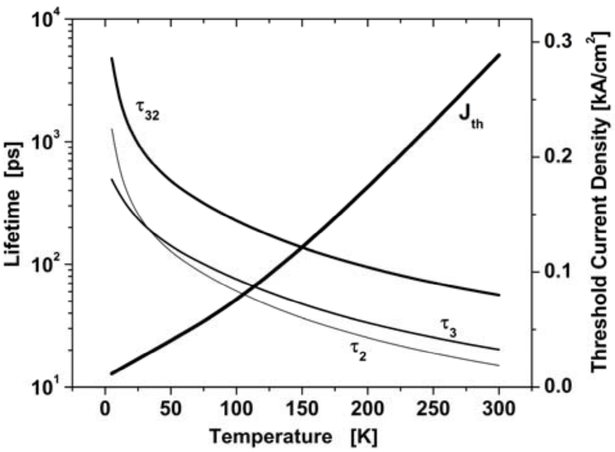

Fig. 2. Lifetimes and threshold current density as a function of temperature.

We have calculated the threshold current density J_{th} from the relation, $\Gamma g = \alpha$, where Γ is the optical confinement factor and α is the total loss including waveguide and mirror losses. Using values of $\Gamma = 0.8$ and α=50/cm for a typical 1 mm QCL cavity, we obtain J_{th} as a function of operating temperature (Fig.2) that ranges from 0.012 kA/ cm^2 at 5K to 0.289 kA/ cm^2 at 300K.

REFERENCES

[1] G. Sun, L. Friedman, and R. A. Soref, Appl. Phys. Lett. **66**, 3425 (1995)
[2] G. Dehlinger, L. Diehl, U. Gennser, H. Sigg, J. Faist, K. Ensslin, D. Grützmacher, and E. Müller, Science **290**, 2277 (2000)
[3] I. Bormann, K. Brunner, S. Hackenbuchner, G. Abstraiter, S. Schmult, and W. Wegscheider, Appl. Phys. Lett. **80**, 2260 (2002)
[4] S. A. Lynch, R. Bates, D. J. Paul, D. J. Norris, A. G. Cullis, Z. Ikonić, R. W. Kelsall, P. Harrison, D. D. Arnone, and C. R. Pidgeon, Appl. Phys. Lett. **81**, 1543 (2002)
[5] K. Driscoll and R. Paiella, Appl. Phys. Lett. **89**, 191110 (2006)
[6] R. A. Soref and C. H. Perry, J. Appl. Phys. **69**, 539 (1991)
[7] D. W. Jenkins and J. D. Dow, Phys. Rev. B **36**, 7994 (1987)
[8] G. He and H. A. Atwater, Phys. Rev. Lett. **79**, 1937 (1997)
[9] J. Menéndez and J. Kouvetakis, Appl. Phys. Lett. **85**, 1175 (2004)
[10] M. Bauer, C. Ritter, P. A. Crozier, J. Ren, J. Menéndez, G. Wolf, and J. Kouvetakis, Appl. Phys. Lett. **83**, 2163 (2003)